Proceedings of the International Symposium on Engineering Lessons Learned from
the 2011 Great East Japan Earthquake, March 1-4, 2012, Tokyo, Japan

DAMAGE ASSESSMENT ON ROAD STRUCTURES DUE TO SLOPE FAILURES IN THE 2011 OFF THE PACIFIC COAST OF TOHOKU EARTHQUAKE

Toshiaki SAKURAI[1], Gaku SHOJI[2], Kazunori TAKAHASHI[3] and Tomoharu NAKAMURA[4]

[1] Graduate Student, Graduate School of Systems and Information Engineering, University of Tsukuba, Ibaraki, Japan, e0611356@edu.esys.tsukuba.ac.jp
[2] Associate Professor, Faculty of Engineering, Information and Systems, University of Tsukuba, Ibaraki, Japan, gshoji@kz.tsukuba.ac.jp
[3] Graduate Student, Graduate School of Systems and Information Engineering, University of Tsukuba, Ibaraki, Japan, s1120951@u.tsukuba.ac.jp
[4] College of Engineering Systems, University of Tsukuba, Ibaraki, Japan, e0811237@edu.esys.tsukuba.ac.jp

ABSTRACT: The damage on road structures due to slope failures in the 2011 off the Pacific Coast of Tohoku earthquake is assessed. We classify 13 types of failure modes for 43 data and analyze them from view of points of dependency of the damage on spatial distributions of peak ground acceleration, peak ground velocity, and seismic intensity induced by the earthquake. Previously proposed damage functions on the failures of road structures due to slope failures in the 2008 Iwate-Miyagi Nairiku earthquake are verified by comparing the derived results with the values from the damage functions.

Key Words: The 2011 off the Pacific Coast of Tohoku earthquake, the 2008 Iwate-Miyagi Nairiku earthquake, slope failure, road structure, damage function

INTRODUCTION

Road structures were damaged severely in the 2011 off the Pacific Coast of Tohoku earthquake (M_{JMA}=9.0) (JMA 2011a) due to not only tsunami waves, but also induced ground excitations. The ground excitations caused the slope failures in mountainous areas which induce various types of damage of road structures. The related researchers and practitioners paid intended attention to the damage of infrastructures such as road structures due to slope failures during strong ground excitations in previous extreme earthquakes such as the 2008 Iwate-Miyagi Nairiku earthquake (M_{JMA}=7.2) (Joint Survey Team of JSCE, JGS, JAEE, and the Japan Landslide Society 2008) and the 2008 Wenchuan earthquake, China (M_w=7.9) (USGS 2008) (Chigira 2005, Hunag et al. 2007, Nishida et al. 2007, Fujiwara et al. 2008, Tamakoshi 2008, Kokusho et al. 2009, Konagai et al. 2009, Nishiki et al. 2009, and Zhang et al. 2009). In these earthquakes, pavement of road structures were suffered and cut slopes of road structures were collapsed due to slope failures by ground shakings. Previous studies were involved in clarifying mechanism of occurrence of slope failures during an earthquake and in

Table 1 Analyzed data of damaged road structures

Road Management Sectors	Damage Information (URL)	Road Management Sectors	Damage Information (URL)
Tohoku Regional Development Bureau Main Office	【Disasiter Prevention Imformation】(Press Release) Tohoku Regional Development Bureau Earthquake Imformation (15th Version) http://www.thr.mlit.go.jp/bumon/kisya/saigai/sback/zokuhou1110.htm	Kanto Regional Development Bureau Omiya National Road Office	Road Damage Information in the 2011 off the Pacific Coast of Tohoku Earthquake (1st and 3rd Versions) http://www.ktr.mlit.go.jp/oomiya/04data/kisha/h22.htm
Tohoku Regional Development Bureau Iwate River and National Road Office	Earthquake Imformation : Iwate River and National Road Office (2nd and 3rd Versions) http://www.thr.mlit.go.jp/iwate/bousai/bousai/index.htm	Kanto Regional Development Bureau Shuto National Road Office	Damage of National Road No. 298 (18:50 on March 11) http://www.ktr.mlit.go.jp/syuto/index.htm
Tohoku Regional Development Bureau Sanriku National Road Office	Sanriku National Road Office Earthquake Imformation (2nd Version) http://www.thr.mlit.go.jp/sanriku/index.html	Kanto Regional Development Bureau Yokohama National Road Office	Damage Imformation in the 2011 off the Pacific Coast of Tohoku Earthquake (3rd Version) http://www.ktr.mlit.go.jp/yokohama/report/bn2010.htm
Tohoku Regional Development Bureau Sendai River and National Road Office	【Disasiter Prevention Imformation】 (Press Release) Sendai River and National Road Office Disaster Information (3rd, 13th, and 14th Versions) http://www.thr.mlit.go.jp/sendai/index.html	Aomori Prefecture	Disaster Countermeasures Office About the Damage in the 2011 off the Pacific Coast of Tohoku Earthquake (43th Version) http://www.pref.aomori.lg.jp/
Tohoku Regional Development Bureau Yamagata River and National Road Office	【Disasiter Prevention Imformation】 Yamagata River and National Road Office Earthquake Imformation (3rd, 4th, 6th, and 7th Versions) http://www.thr.mlit.go.jp/bumon/kisya/saigai/sback/zokuhou1106.htm	Iwate Prefecture	Situation of Road Traffic Regulation Management due to the Earthquake in Iwate Prefecture on March 11 (As of 9:30 on August 12) http://www.pref.iwate.jp/list.rbz?nd=2974&ik=1&pnp=2974&of=13
Tohoku Regional Development Bureau Fukushima River and National Road Office	【Disasiter Prevention Imformation】Fukushima River and National Road Office Earthquake Imformation (8th Version) http://www.thr.mlit.go.jp/fukushima/pressedit/disaster_index.html	Akita Prefecture	Imformation Earthquake (2nd, 4th, 5th, 6th, and 9th Versions) http://www.pref.akita.lg.jp/www/genre/0000000000000/1243242791775/index.html
Tohoku Regional Development Bureau Koriyama National Road Office	【Disasiter Prevention Imformation】 Koriyama National Road Office : Emergency System Response in the 2011 off the Pacific Coast of Tohoku Earthquake (2nd, 8th, and 20th Versions) http://www.thr.mlit.go.jp/bumon/kisya/saigai/sback/zokuhou1117.htm	Miyagi Prefecture	Traffic Regulation in the 2011 off the Pacific Coast of Tohoku Earthquake (As of 16:00 on May 8) http://www.pref.miyagi.jp/road/kiseinow.htm Damag of Public Facility and Emergency Disaster Recovery Situations in the 2011 off the Pacific Coast of Tohoku Earthquake (Updated August 10) http://www.pref.miyagi.jp/doboku/110311dbk_taiou/index.htm
Tohoku Regional Development Bureau Banjyo National Road Office	【Disasiter Prevention Imformation】 Banjyo National Road Office : Road Disasiter Prevention Imformation Earthquake (5th Version) http://www.thr.mlit.go.jp/bumon/kisya/saigai/sback/zokuhou1132.htm	Yamagata Prefecture	(Press Release) The 2011 off the Pacific Coast of Tohoku Earthquake (3rd and 10th Versions) http://www.pref.yamagata.jp/
Kanto Regional Development Bureau Main Office	Road Division at Kanto Regional Development Bureau Disaster Imformation of National Road in the 2011 off the Pacific Coast of Tohoku Earthquake (15:00 on March 18, 2011) http://www.ktr.mlit.go.jp/saigai/kyoku_dis00000021.html	East Nippon Expressway Company Limited	Damaged Routes and Sections (List) (March 18) http://www.e-nexco.co.jp/whatsnew/h22.html
Kanto Regional Development Bureau Hitachi River and National Road Office	Hitachi River and National Road Office (Press release) : Announcement for the Damage due to the 2011 off the Pacific Coast of Tohoku Earthquake (10:30 on March 12, 2011) http://www.ktr.mlit.go.jp/kisha/index00000022.html	Metropolitan Expressway Company Limited	(Press Release) Influence and Emergency Response due to the 2011 off the Pacific Coast of Tohoku Earthquake and Correspondence (March 14, 2011) http://www.shutoko.jp/
Kanto Regional Development Bureau Utsunomiya National Road Office	Road Damage Information for the 2011 off the Pacific Coast of Tohoku Earthquake (17:00 on March 11, 18:30 on March 11, 12:00 on March 12) http://www.ktr.mlit.go.jp/utunomiya/bousai/old.htm	—	—

clarifying the dependency of damage of road structures on occurrence of slope failures. Based on previous valuable results, we analyzed damage data on road structures due to slope failures in the 2011

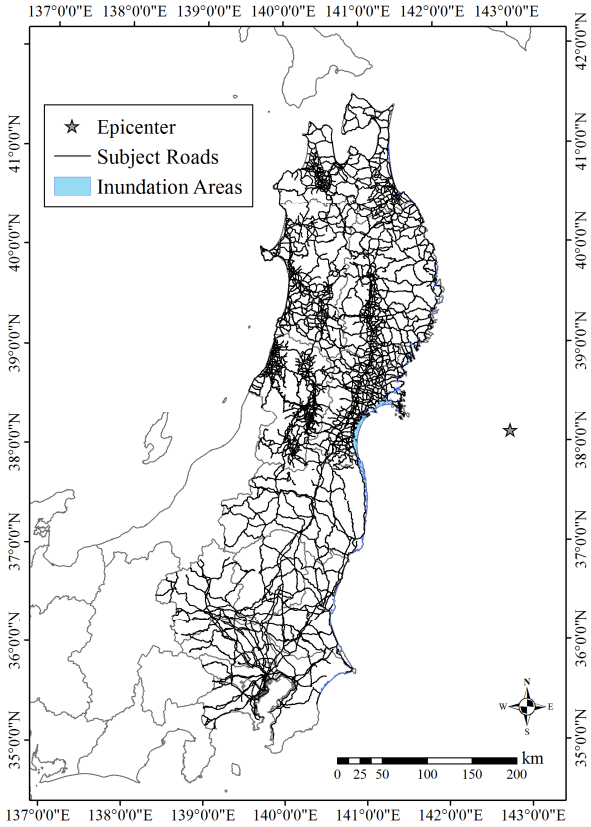

Fig. 1 Subject roads without inundation areas

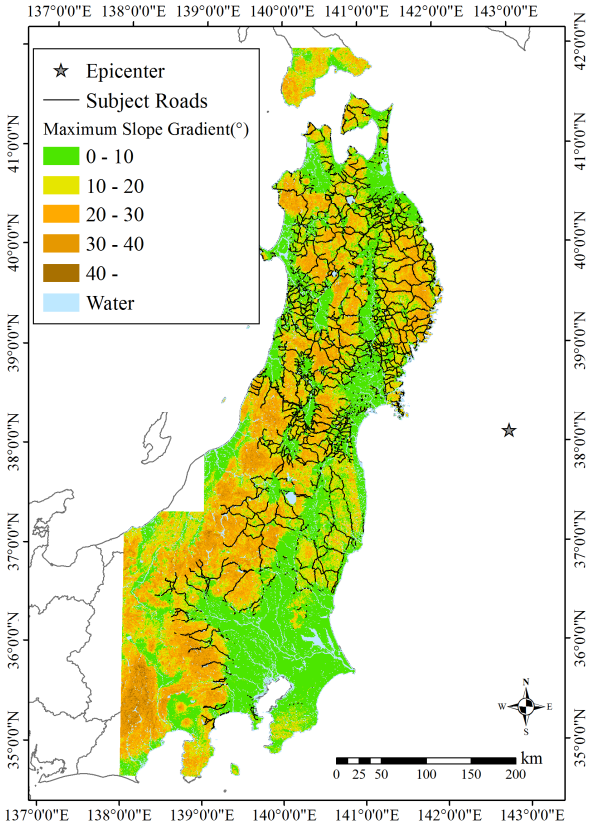

Fig. 2 Subject roads for analysis

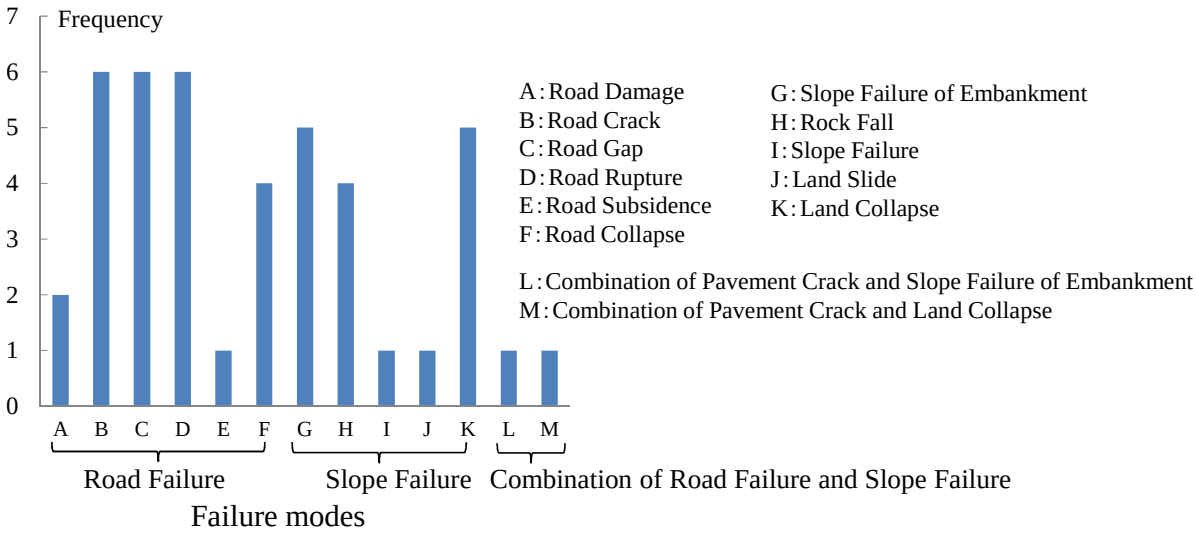

Fig. 3 Induced failure modes

off the Pacific Coast of Tohoku earthquake (hereinafter the Tohoku earthquake) and clarified the relationship of related damage ratios with spatial distributions of peak ground acceleration (*PGA*), peak ground velocity (*PGV*), and instrumental seismic intensity (*IJ*). In addition, damage functions on the failures of road structures due to slope failures in the 2008 Iwate-Miyagi Nairiku earthquake (hereinafter the Iwate-Miyagi Nairiku earthquake), proposed by Shoji and Sakurai (2011), are verified by comparing the derived results from this study with the values from the damage functions.

SUBJECT ROAD STRUCTURES AND THE DAMAGE MODES

Analyzed data of damaged road structures

Damage data of road structures due to slope failures except damage data of bridges and tunnels are analyzed. Analyzed road structures are national roads at six prefectures of Tohoku regions, Tokyo metropolitan areas and six prefectures of Kanto regions by Tohoku Regional Development Bureau, Kanto Regional Development Bureau, East Nippon Expressway Company Limited and Metropolitan Expressway Company Limited, and prefectural roads at five prefectures of Tohoku regions without Fukushima prefecture by local government sectors. Table 1 shows the information of damaged road structures which is opened at the related web sites by road management authorities and local government sectors. Total number of the data is 680. For selecting 680 data, we removed the damage data to be possibly affected by the ground motions due to the aftershocks after March 11, 2011.

Based on the data, first, we identified the locations of damaged road structures. Second, we removed 158 data as the data subjected to the tsunami waves by comparing the locations of damaged road structures with estimated inundation areas by GSI (2011) and selected 522 data as those dominantly exposed by the ground excitations.

Among 522 data, the exact locations of 360 data offered by East Nippon Expressway Company Limited cannot be clarified since these data show the number of damage points between any interchanges. Therefore, we removed above 360 data and set 162 data as analyzed ones. For 162 data, finally we focused on 43 data which are assumed to be affected by slope failures in subject areas showing maximum slope gradients equal to or over 10 degrees (Ishide and Yamazaki 2010). Furthermore, in order to verify validness of occurrence of slope failures and induced damage at subject road structures, we check all image data for 43 data by Google Earth.

We model subjected roads without estimated inundation areas by GSI as shown in Fig. 1, by using the digital data of national roads and major prefectural roads in 6 prefectures of Tohoku regions, Tokyo Metropolitan areas and 6 prefectures of Kanto regions offered by National and Regional Planning Bureau (2011) and by constructing the digital data of other prefectural roads in 5 prefectures of Tohoku regions except Fukushima prefecture by checking Google Earth. In addition, among above roads, we select the roads with slopes showing maximum slope gradients equal to or over 10 degrees as shown in Fig. 2. Again we checked the locations of roads with slopes by Google Earth. Total length of subject roads is 14,258km.

Damage modes

Fig. 3 shows 13 failure modes: 6 road failure modes, 5 slope failure modes, and 2 combination failure modes of road failure and slope failure. 25 data on road failure modes are classified into 6 failure modes: 6 data for road crack, 6 data for road gap, 6 data for road rupture, 4 data for road collapse, and others. 16 data on slope failure modes are classified into 5 failure modes: 5 data for failure of embankment slope, 5 data for land collapse, 4 data for rock fall, and others.

DAMAGE ASSESMENT FOR SUBJECT ROAD STRUCTURES

Evaluation of spatial distributions of *PGA*, *PGV*, and *IJ*

Fig. 4 shows estimated spatial distributions with a 250m-mesh of *PGA*, *PGV*, and *IJ* for analysis, based on the simple kriging method by using 535 observation waveforms by K-NET and KiK-net (NIED 2011), and 44 observation waveforms by JMA (2011b) as shown in Fig. 5. These observatory stations are distributed at Aomori, Akita, Yamagata, Iwate, Miyagi, Fukushima, Ibaraki, Tochigi, Gunma, Chiba, Saitama, Yamanashi, Nagano, and Niigata prefectures, and Tokyo Metropolitan areas. We describe the procedures of computing the distributions of *PGA*, *PGV*, and *IJ* in the followings.

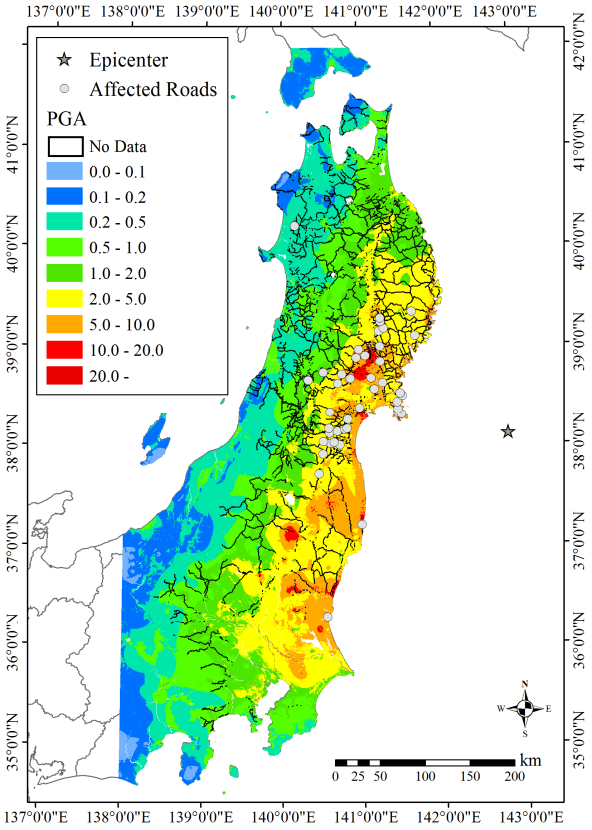

(a) P*GA* distribution

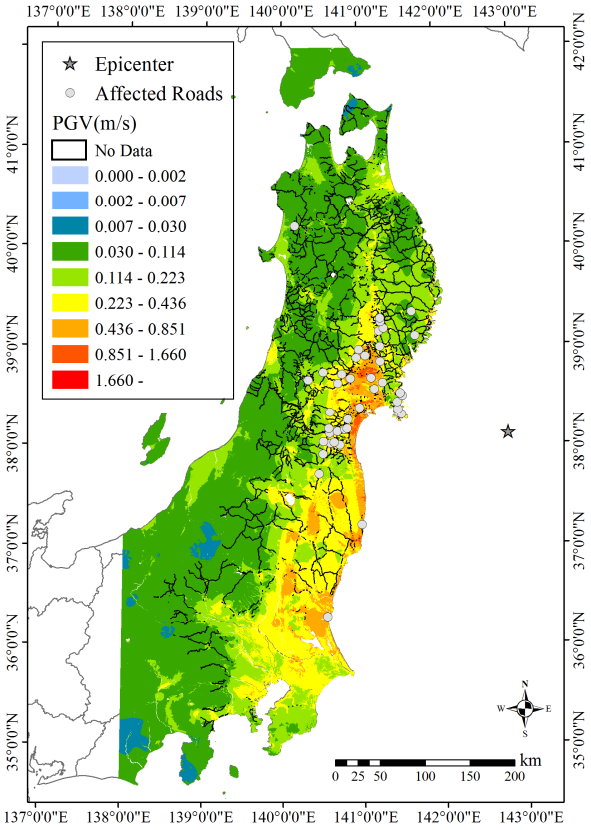

(b) *PGV* distribution

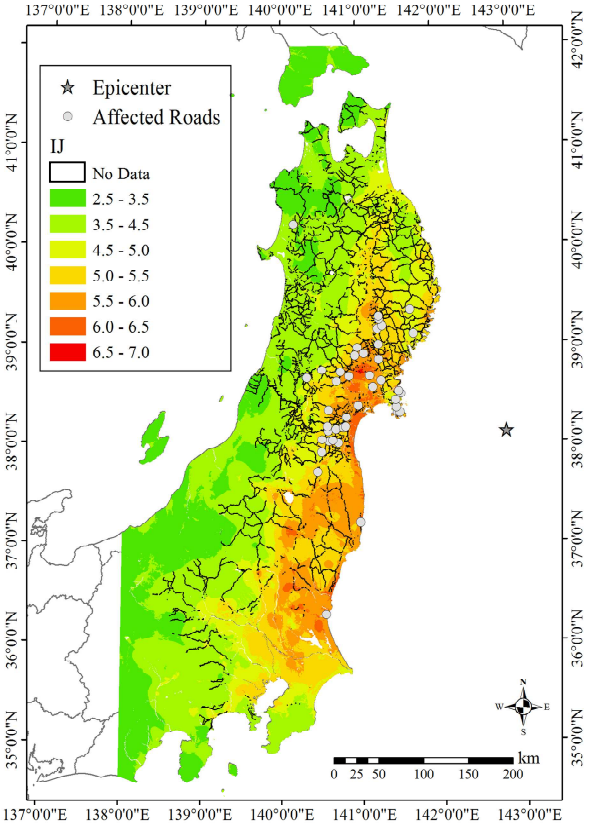

(c) *IJ* distribution

Fig. 4 Spatial distributions of affected roads and *PGA*, P*GV*, and *IJ*

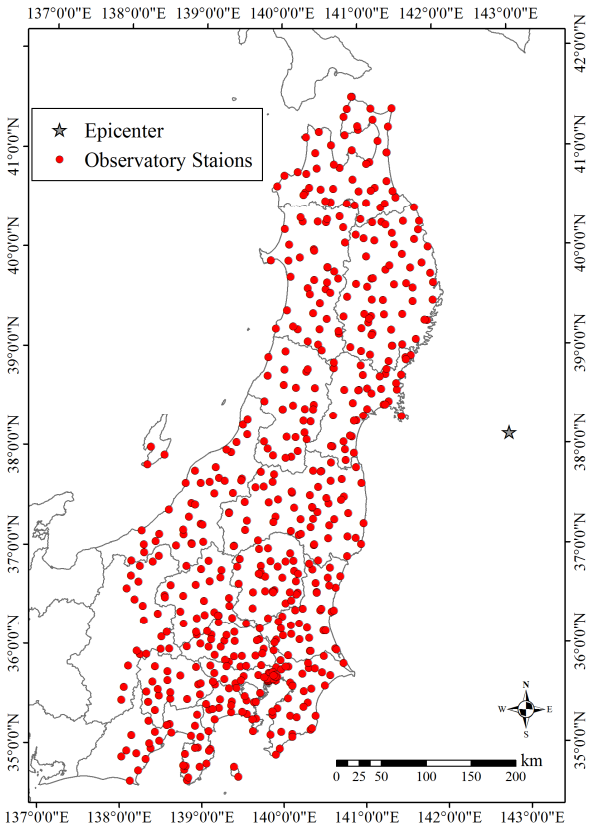

Fig. 5 Observatory stations for analysis

First, *PGA* at an arbitrary station is computed by selecting maximum value in a time history composing EW, NS, and UD components of an observed waveform. We calibrate the time history data by subducting mean value from the data recorded by K-NET and KiK-net. We compute PGA_{b600} at a base level with average *S* wave velocity *Vs* of 600m/s by applying the related factors α, β on amplification of *PGA* at a ground surface compared with PGA_{b600}. The amplification factors α, β are obtained by the following equations proposed by Suetomi et al. (2005),

$$\left.\begin{aligned} X_S &= \alpha \cdot X_b && (X_b \le X_1) \\ X_S &= X_L - \beta \cdot (X_b - X_2) && (X_1 < X_b < X_2) \\ X_2 &= \frac{2}{\alpha} X_L - X \\ \beta &= \frac{X_L - \alpha \cdot X_1}{(X_2 - X_1)^2} \\ X_S &= X_L && (X_b \ge X_2) \end{aligned}\right\} \quad (1)$$

$$\log(\alpha) = 2.024 - 0.75 \cdot \log(AVS20) \quad (2)$$

$$\log(X_1) = 1.4 \cdot \log(AVS20) - 0.8 \quad (3)$$

$$\log(X_L) = 1.0 \cdot \log(AVS20) + 0.778 \quad (4)$$

Now, in Eq. (1) to Eq. (4), we set X_S=*PGA* and X_b=PGA_{b600}, and interpret X_1 and X_2 as the threshold values describing the relation between X_S and X_b dependent on classification of subject ground condition. *AVS*20 is an average *S* wave velocity at a layer of 20m under a ground surface, and computed by the following equation proposed by Kanno et al. (2006),

$$AVS30 = 1.13AVS20 + 19.5 \tag{5}$$

where *AVS*30 is similarly average *S* wave velocity at a layer of 30m under a ground surface, and we obtain the value with a 250m-mesh from the data of geomorphologic classification (Matsuoka et al. 2005). By using estimated PGA_{b600} data at observatory stations, we compute PGA_{b600} with a 250m-mesh based on simple kriging interpolation. We use attenuation relationship between PGA_{b600} and minimum distance from an arbitrary site to a fault plate *R* proposed by Shi and Midorikawa (1999), for evaluating the mean trend component in adopting simple kriging method as shown in the following equation,

$$Log_{10}PGA_{b600} = c_1 - Log_{10}(R + c_2) + c_3 \tag{6}$$

where *c*1, *c*2, and *c*3 are recurrence constants obtained by the least squares method. In addition, for evaluating the variance in adopting simple kriging method, we use exponential model as a covariance model,

$$\gamma = Var[PGA_{b600}{}^2]\exp^{(-h/a)} \tag{7}$$

where γ is the covariance of PGA_{b600}, *h* is the distance between an arbitrary site with a 250m-mesh and the observatory station, and *a* is the correlation distance. We set *a*=40km for which the variation of spatial distributions of *PGA* converges when *a* varies for 20km, 30km, 40km, and 50km.

PGV at an arbitrary station is computed by selecting maximum value in a time history composing two horizontal EW and NS components of an observed waveform integrated by acceleration EW and NS waveforms with filtering by Bata Worth high pass filter with lowest cut-off frequency of 0.05Hz and pass frequency of 0.1Hz for K-NET and KiK-net waveforms, and with filtering of cut-off frequency equal to or less than 0.2Hz by using the integration recurrence formula for JMA waveforms. We compute PGV_{b600} at a base level with average *S* wave velocity *Vs* of 600m/s by applying the related factor *ARV* on amplification of *PGV* at a ground surface compared with PGV_{b600}. The relation of PGV_{b600} with *PGV* is obtained by the following equations proposed by Fujimoto and Midorikawa (2006),

$$PGV_{b600} = PGV / ARV \tag{8}$$

$$Log_{10}ARV = 2.367 - 0.852Log_{10}AVS30 \tag{9}$$

By using estimated PGV_{b600} data at observatory stations, we compute PGV_{b600} with a 250m-mesh based on simple kriging interpolation. We use attenuation relationship between PGV_{b600} and *R* proposed by Shi and Midorkawa (1999), for evaluating the mean trend component in adopting Simple Kriging method as well as for computation of *PGA*. In addition, for evaluating the variance in adopting simple kriging method, we use exponential model as a covariance model. We set *a*=40km for which the variation of spatial distribution of *PGV* converges when *a* varies for 20km, 30km, 40km, and 50km.

IJ at an arbitrary station is computed by computational scheme by JMA (2011c). We compute IJ_{b600} at a base level with average *S* wave velocity *Vs* of 600m/s by applying the related factors α, β on amplification of *IJ* at a ground surface compared with IJ_{b600}. The amplification factors α, β are obtained by the following equations proposed by Suetomi et al. (2005),

$$\left.\begin{aligned} \lambda_{IJ} &= \alpha_{IJ} && \left(IJ_b \le IJ_1\right) \\ \lambda_{IJ} &= \alpha_{IJ} - \beta \cdot \left(IJ_b - IJ_1\right) && \left(IJ_1 < IJ_b < IJ_2\right) \\ \beta_{IJ} &= \frac{\alpha_{IJ} - IJ_L + IJ_2}{IJ_2 - IJ_1} \\ \lambda_{IJ} &= IJ_L - IJ_b && \left(IJ_2 \le IJ_b\right) \end{aligned}\right\} \quad (10)$$

$$\alpha_{IJ} = 2.699 - \log\left(AVS20\right) \quad (11)$$

$$IJ_1 = 0.8 + 2.25 \cdot \log\left(AVS20\right) \quad (12)$$

$$IJ_2 = 1.15 + 2.4 \cdot \log\left(AVS20\right) \quad (13)$$

$$IJ_L = 2.2 + 2.0 \cdot \log\left(AVS20\right) \quad (14)$$

By using estimated IJ_{b600} data at observatory stations, we compute IJ_{b600} with a 250m-mesh based on simple kriging interpolation. We apply same procedures for evaluating the mean trend component and variance in adopting simple kriging method, and for setting the correlation distance *a* as well as the procedures for computation of spatial distributions of *PGA* and *PGV*.

We verify the derived spatial distributions of *PGA*, *PGV*, and *IJ* from above procedures with same spatial distributions computed by NIED (2011), JMA (2011a), Suetomi and Fukushima (2011), and AIST (2011), and we check the agreement of our results with the reference results.

Relations of damage ratio with *PGA*, *PGV*, and *IJ*

Fig. 6 shows the relations between road damage and spatial distributions of *PGA*, *PGV*, and *IJ*. Now, we define damage ratio *R* as the ratio of the number of damage points *X* divided by total exposed road lengths *L* in an unit of kilometer. For damage ratio *R* with *PGA* of 0m/s^2 to 20m/s^2, the interval of *PGA* is set as 0.5m/s^2, for *R* with *PGV* of 0.01m/s to 1.4m/s, the interval of *PGV* is set as 0.01m/s, and for *R* with *IJ* of 2.5 to 6.7, the interval of *IJ* is set as 0.1.

From Fig. 6(a), *R* with *PGA* of 0.5m/s^2 shows the minimum value of 0.000264/km at the lowest limit of *PGA* and *R* with *PGA* of 11.5m/s^2 shows the maximum value of 0.0589/km. *R* with *PGA* of 1.5m/s^2 to 3.0m/s^2 increases the value of 0.000637/km to 0.00333/km, *R* with *PGA* of 3.0m/s^2 to 7.0m/s^2 increases the value of 0.00264/km to 0.0316/km, and *R* with *PGA* of 9.0m/s^2 to 11.5m/s^2 increases the value of 0.0229/km to 0.0589/km. In contrast, *R* with *PGA* over 12m/s^2 shows zero in spite of becoming higher *PGA*. This is because the possibility of occurrence of road damage becomes low with shortening exposed road lengths less than 17.7km.

From Fig. 6(b), *R* with *PGV* of 0.1m/s shows the minimum value of 0.00239/km at the lowest limit of *PGV* and *R* with *PGV* of 0.62m/s shows the maximum value of 0.0687/km. *R* with *PGV* of 0.1m/s to 0.3m/s increases the value of 0.00239/km to 0.0202/km, *R* with *PGV* of 0.3m/s to 0.5m/s increases the value of 0.00964/km to 0.0508/km, and *R* with *PGV* of 0.5m/s to 0.62m/s increases the value of 0.0312/km to 0.0687/km. *R* with *PGV* over 0.63m/s shows zero in spite of becoming higher *PGV*, that is caused by same reason for higher *PGA* over 12m/s^2.

From Fig. 6(c), *R* with *IJ* of 3.7 shows the lower value of 0.00169/km at the lowest limit of *IJ* and *R* with *IJ* of 5.9 shows the maximum value of 0.0226/km. *R* with *IJ* of 4.5 to 5.0 increases the value of 0.00176/km to 0.00401/km, *R* with *IJ* of 5.0 to 5.5 increases the value of 0.00157/km to 0.0139/km, and *R* with *IJ* of 5.5 to 5.9 increases the value of 0.00690/km to 0.0226/km. Similarly, *R* with *IJ* over 6.0 shows zero in spite of becoming higher *IJ*.

Comparison of analyzed data with previous damage functions

Fig. 7 shows the comparison of analyzed data for the Tohoku earthquake with damage ratios for the Iwate-Miyagi Nairiku earthquake data and damage functions by the Iwate-Miyagi Nairiku earthquake data proposed by Shoji and Sakurai (2011).

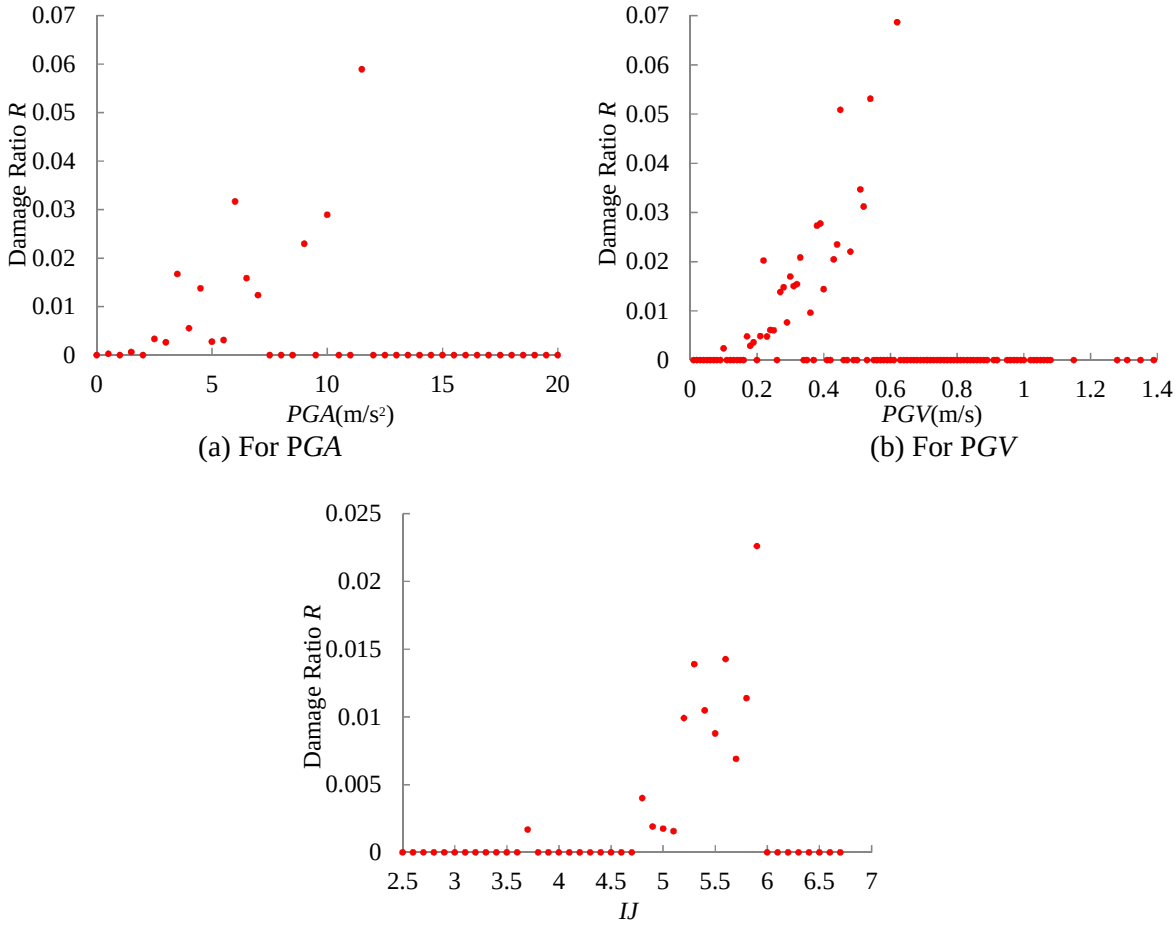

(a) For P*GA* (b) For P*GV*

(c) For *IJ*

Fig. 7 Comparison of the damage ratio for *PGA*, *PGV*, and *IJ*

From Fig. 7(a), averaged values of difference from observed data for the Iwate-Miyagi Nairiku earthquake to analyzed data for the Tohoku earthquake with *PGA* of 3.0m/s^2 to 6.0m/s^2 shows 0.038/km and those with *PGA* of 6.0m/s^2 to 10m/s^2 at higher *PGA* becomes the larger value of 0.13/km. Averaged values of difference from the values by damage function to analyzed data for the Tohoku earthquake with *PGA* of 3.0m/s^2 to 6.0m/s^2 shows 0.036/km and those with *PGA* of 6.0m/s^2 to 10m/s^2 at higher *PGA* shows the larger value of 0.18/km. In the above, *R* with relatively lower *PGA* of 3.0m/s^2 to 6.0m/s^2 shows the narrow differences. In contrast, *R* with relatively higher *PGA* of 6.0m/s^2 to 10m/s^2 shows the wider differences.

From Fig. 7(b), averaged values of difference from observed data for the Iwate-Miyagi Nairiku earthquake to analyzed data for the Tohoku earthquake with *PGV* of 0.1m/s to 0.3m/s shows 0.052/km and those with *PGV* of 0.5m/s to 0.6m/s shows the larger value of 0.22/km. Averaged values of difference from the values by damage function to analyzed data for the Tohoku earthquake with *PGV* of 0.1m/s to 0.3m/s shows 0.0043/km and those with *PGV* of 0.5m/s to 0.6m/s shows the larger of 0.17/km. In the above, *R* with relatively lower *PGV* of 0.1m/s to 0.3m/s shows the narrow differences. In contrast, *R* with relatively higher *PGV* of 0.5m/s to 0.6m/s shows the larger wider differences.

From Fig. 7(c), averaged values of difference from observed data for the Iwate-Miyagi Nairiku earthquake to analyzed data for the Tohoku earthquake with *IJ* of 4.5 to 5.5 shows 0.024/km and those with *IJ* of 5.5 to 6.5 shows the larger value of 0.26/km. Averaged values of difference from the values by damage function to analyzed data for the Tohoku earthquake with *IJ* of 4.5 to 5.5 shows 0.017/km and those with *IJ* of 5.5 to 6.5 shows the larger value of 0.29/km. In the above, *R* with relatively lower *IJ* of 4.5 to 5.5 shows the narrow differences. In contrast, *R* with relatively higher *IJ* of 4.5 to 5.5 shows the larger wider differences.

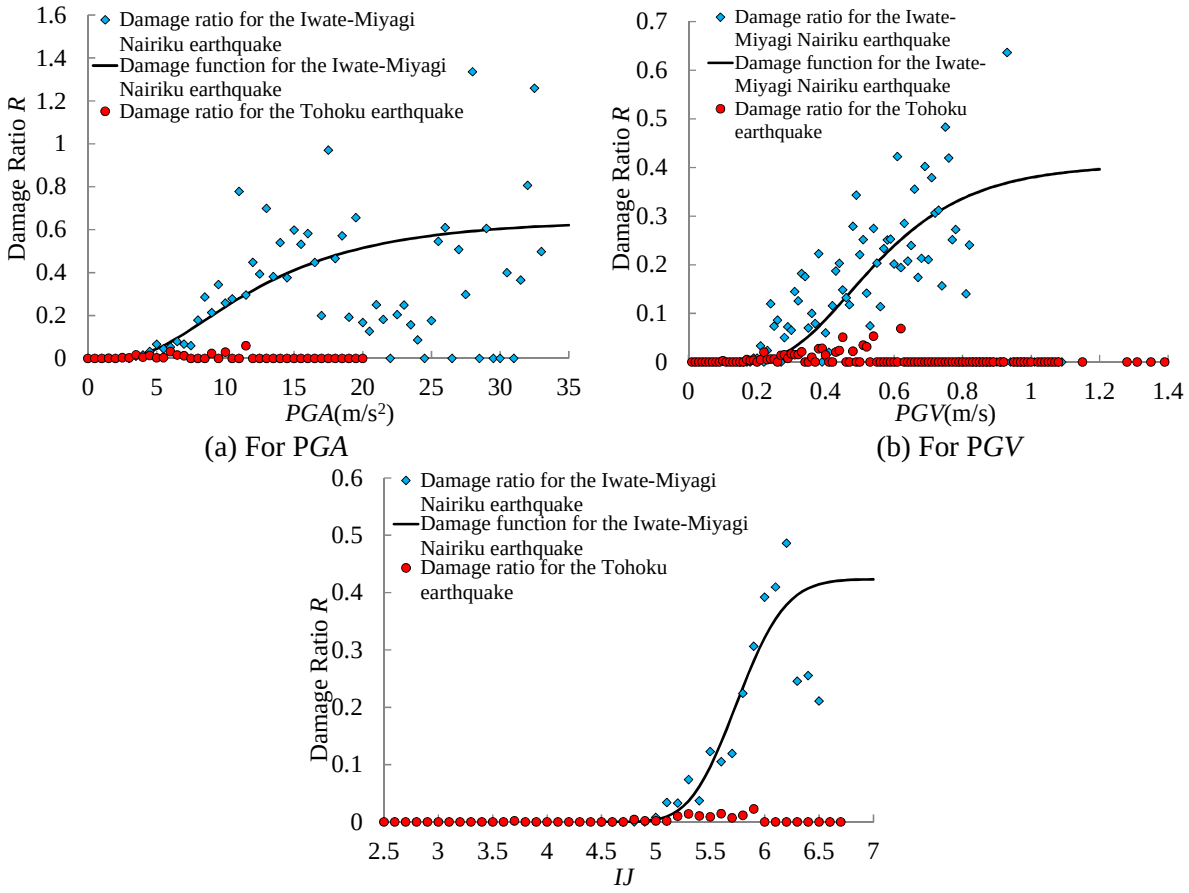

(a) For P*GA* (b) For P*GV*

(c) For *IJ*

Fig. 6 Comparison of analyzed data for the Tohoku earthquake with damage ratios for the Iwate-Miyagi Nairiku earthquake data and damage functions by the Iwate-Miyagi Nairiku earthquake data

Hence, ground excitations with *PGA* of 6.0m/s^2 to 10m/s^2, *PGV* of 0.5m/s to 0.6m/s, and *IJ* of 4.5 to 5.5 for the Iwate-Miyagi Nairiku earthquake induced larger damage of road structures due to slope failures than those with same ranges of *PGA*, *PGV*, and *IJ* for the Tohoku earthquake.

CONCLUSIONS

We analyzed damage data on road structures due to slope failures in the 2011 off the Pacific Coast of Tohoku earthquake and clarified the relationship of related damage ratios with spatial distributions of peak ground acceleration (*PGA*), peak ground velocity (*PGV*), and instrumental seismic intensity (*IJ*). In addition, previously proposed damage functions on the failures of road structures due to slope failures in the 2008 Iwate-Miyagi Nairiku earthquake are verified by comparing the derived results from this study with the values from the damage functions.

(1) The failure modes are classified for 43 data on the damage of road structures due to slope failures into 13 failure modes: 6 road failure modes, 5 slope failure modes, and 2 combination failure modes of road failure and slope failure. 25 data on road failure modes are classified into 6 failure modes: 6 data for road crack, 6 data for road gap, 6 data for road rupture, 4 data for road collapse, and others. 16 data on slope failure modes are classified into 5 failure modes: 5 data for failures of embankment slope, 5 data for land collapse, 4 data for rock fall, and others.

(2) Damage ratio *R* was defined as the ratio of the number of damage points *X* divided by total exposed road lengths *L* in an unit of kilometer. *R* with *PGA* of 0.5m/s^2 shows the minimum value of 0.000264/km at the lowest limit of *PGA* and *R* with *PGA* of 11.5m/s^2 shows the maximum value

of 0.0589/km. *R* with *PGV* of 0.1m/s shows the minimum value of 0.00239/km at the lowest limit of *PGV* and *R* with *PGV* of 0.62m/s shows the maximum value of 0.0687/km. *R* with *IJ* of 3.7 shows the lower value of 0.00169/km at the lowest limit of *IJ* and *R* with *IJ* of 5.9 shows the maximum value of 0.0226/km.

(3) Ground excitations with *PGA* of 6.0m/s^2 to 10m/s^2, *PGV* of 0.5m/s to 0.6m/s, and *IJ* of 4.5 to 5.5 for the Iwate-Miyagi Nairiku earthquake induced larger damage of road structures due to slope failures than those with same ranges of *PGA*, *PGV*, and *IJ* for the Tohoku earthquake.

ACKNOWLEDGMENTS

We appreciate valuable supports for modeling of damage functions from Professor Yamada Y. and Professor Matsushima T. at University of Tsukuba, and also appreciate valuable cooperation for calculating of spatial distributions of *PGA*, *PGV*, and *IJ* from Mr. Kado S. and Mr. Hang Q. at University of Tsukuba.

REFERENCES

Chigira, M. (2005). "Geological and geomorphological characteristics of landslides generated by the mid Niigata prefecture earthquake in 2004." *Jour. Japan Soc. Eng. Geol.*, Vol.46, No.3, 115-124.

Fujimoto, K. and Midorikawa, S. (2006). "Relationship between average shear-wave velocity and site amplification inferred from strong motion records at nearby station pairs." *Journal of Japan Association for Earthquake Engineering*, Vol.6, No.1, 11-22.

Fujiwara, T., Taketani, T., Imai, T. and Mizuno, K. (2008). "Case study of the process of slope failure at the Oumigawa station caused by the Niigataken Chuetsu-Oki earthquake in 2007." *The 43th Japan National Conference on Geotechnical Engineering*, No.859/H-06, 1717-1718.

Geospatial Information Authority of Japan (GSI) (2011). "Digital Elevation Model." http://www.gsi.go.jp/kiban/etsuran.html.

Hunag, Y., Sakajo, S., Sadamura, T. and Nishioka, T. (2007). "Analysis of some factors to induce land collapse in Hyogoken-nanbu earthquake." *The 42th Japan National Conference on Geotechnical Engineering*, No.1020/C-09, 2033-2034.

Ishide, T. and Yamazaki F. (2010). "Detection of slope failures using ALOS/AVNIR-2 images for the 2008 Iwate-Miyagi inland earthquake." *Journal of Japan Association for Earthquake Engineering*, Vol.10, No.3, 12-24.

Japan Meteorological Agency (JMA) (2011a). "Earthquake Information in the 2011 off the Pacific Coast of Tohoku earthquake." http://www.seisvol.kishou.go.jp/eq/2011_03_11_tohoku/index.html.

Japan Meteorological Agency (JMA) (2011b). "Observatory stations for the Tohoku earthquake." http://www.seisvol.kishou.go.jp/eq/kyoshin/jishin/110311_tohokuchiho-taiheiyouoki/index.html.

Japan Meteorological Agency (JMA) (2011c). "Procedure of calculating instrumental seismic intensity." http://www.seisvol.kishou.go.jp/eq/kyoshin/kaisetsu/calc_sindo.htm.

Joint Survey Team of Japan Society of Civil Engineers (JSCE), Japanese Geotechnical Society (JGS), Japan Association for Earthquake Engineering (JAEE), and the Japan Landslide Society (2008). "Earthquake Information in the 2008 Iwate-Miyagi Nairiku Earthquake." http://www.jsce.or.jp/report/50/news3.shtml.

Kanno, T., Narita, A., Morikawa, N., Fujiwara, H. and Fukushima, Y. (2006). "A new attenuation relation for strong ground motion in Japan based on recorded data." *Bull. Seism. Soc. Am.*, Vol.96, No.3, 879-897.

Kokusho, T., Ishizawa, T., Hase, Y. and Yamamoto, Y. (2009). "Influencing factor of slope failures during 2008 Iwate-Miyagi Nairiku earthquake." *The 44th Japan National Conference on Geotechnical Engineering*, No.717/C-09, 1433-1434.

Konagai, K., eds. (2009). "Investigation report on the May 12th 2008 Wenchuan earthquake, China" *Final Report of the Investigation Project Grant-in-Aid for Special Purposes of 2008, Ministry of*

Education, Culture, Sport, Science and Technology(MEXT), Japan, No.20900002.
Matsuoka, M., Wakamatsu K., Fujimoto, K. and Midorikawa, S. (2005). "Average shear-wave velocity mapping using Japan engineering geomorphologic classification map." *Journal of JSCE*, No.794/I-72, 239-251.
National and Regional Planning Bureau (2011). "National Land Numerical Information download service." http://nlftp.mlit.go.jp/ksj/.
National Institute of Advanced Industrial Science and Technology (AIST) (2011). "QuakeMap." http://qq.ghz.geogrid.org/QuakeMap/.
National Research Institute for Earth Science and Disaster Prevention (NIED) (2011). "K-NET and KiK-net." http://www.kyoshin.bosai.go.jp/kyoshin/.
Nishida, K., Kokusho, T., Ishizawa, T. and Hara, T. (2007). "Statistical study on influencing factors of slope failures during Nigataknen chuetsu earthquake." *JSCE Journal of Earthquake Engineering*, Vol.29, 1117-1122.
Nishiki, Y., Ikemura, H., Shimominami, T., Matsumoto, T. and Kawai, Y. (2009). "Analysis of road embankments during Noto peninsula earthquake in 2007 (part 2: stability analyses)." *The 44th Japan National Conference on Geotechnical Engineering*, No.766/E-06, 1531-1532.
Shi, H. and Midorikawa, S. (1999). "New attenuation relationships for peak ground acceleration and velocity considering effects of fault type and site condition." J. Struct. Constr. Eng., AIJ, No.523, 63-70.
Shoji, G. and Sakurai, T. (2011). "Analysis on failure modes of road structures due to the slope failures in the 2008 Iwate-Miyagi earthquake and development of the related damage function." *Journal of Japan Association for Earthquake Engineering*, Vol.11, No.5, 94-106.
Suetomi, I., Ishida, E. and Isoyama, R. (2005). "A procedure for high-accuracy map of peak ground motion using observed records." *Proc. 28th JSCE Earthquake Engineering Symposium*.
Suetomi, I. and Fukushima, Y. (2011). "Presuming spatial distribution of ground motion in the 2011 off the Pacific Coast of Tohoku earthquake." *The 66th Annual Meeting Proceedings*, I-475, 949-950.
Tamakoshi, T. (2008). "Investigation report in the 2008 Iwate-Miyagi Nairiku earthquake (road bridge)." National Institute for Land and Infrastructure Management (MLIT). http://www.kenken.go.jp/japanese/contents/activities/other/disaster/jishin/2008iwate/houkokusho/20080904-1/07.pdf.
United States Geological Survey (USGS) (2008). "Earthquake Information in the 2008 Wenchuan earthquake." http://earthquake.usgs.gov/eqcenter/eqinthenews/2008/us2008ryan/.
Zhang, J., Zhuang, W., Feng, J., Xiao, S., Ma, H. and Xiang, B. (2009). "Discussions on two technical problems for aseismic design of retaining structures based on investigation of the Wenchuan earthquake." *Proceedings of International Conference on Earthquake Engineering - The First Anniversary of Wenchuan Earthquake*, 82-86.